Role of social interactions in dynamic patterns of resource patches and forager aggregation

Nessy Tania[a], **Ben Vanderlei**[b], **Joel P. Heath**[c], **and Leah Edelstein-Keshet**[c,1]

[a]Department of Mathematics and Statistics, Smith College, Northampton, MA 01063; [b]Department of Mathematics and Statistics, University of the Fraser Valley, Abbotsford, BC, Canada V2S 7M8; and [c]Department of Mathematics, University of British Columbia, Vancouver, BC, Canada V6T 1Z2

Edited by Mark A. Lewis, University of Alberta, Edmonton, Canada, and accepted by the Editorial Board June 4, 2012 (received for review January 31, 2012)

The dynamics of resource patches and species that exploit such patches are of interest to ecologists, conservation biologists, modelers, and mathematicians. Here we consider how social interactions can create unique, evolving patterns in space and time. Whereas simple prey taxis (with consumable prey) promotes spatial uniform distributions, here we show that taxis in producer–scrounger groups can lead to pattern formation. We consider two types of foragers: those that search directly ("producers") and those that exploit other foragers to find food ("scroungers" or exploiters). We show that such groups can sustain fluctuating spatiotemporal patterns, akin to "waves of pursuit." Investigating the relative benefits to the individuals, we observed conditions under which either strategy leads to enhanced success, defined as net food consumption. Foragers that search for food directly have an advantage when food patches are localized. Those that seek aggregations of group mates do better when their ability to track group mates exceeds the foragers' food-sensing acuity. When behavioral switching or reproductive success of the strategies is included, the relative abundance of foragers and exploiters is dynamic over time, in contrast with classic models that predict stable frequencies. Our work shows the importance of considering two-way interaction—i.e., how food distribution both influences and is influenced by social foraging and aggregation of predators.

pattern formation | foraging strategies | ecological patchiness | chemotaxis | spatial ecology

In this paper, we study the dynamics of social interactions to explore the consequences for spatiotemporal population structure and dynamics. We show that interactions among individuals are key for pattern formation and self-organization when foragers either follow gradients of food or socialize with those that do. Our aim is to demonstrate that social interactions among foragers could have particularly important implications for spatial models of forager-resource dynamics. A comprehensive understanding of the spatial dynamics of social foraging needs to consider the two-way dynamic interaction between forager aggregation and resource patchiness, a problem that remains poorly understood (1, 2).

A secondary theme is the discovery of another pattern-forming mechanism. Nature abounds with patterns that the human eye is adept at picking out. Patterns occur in chemical, physical, and biological systems on many scales, from distribution of proteins in a cell, and tissue morphogenesis, to patchy distribution of species in ecology (3–5, 6). There is great interest in finding both universal mechanisms for such patterns (e.g., the balance of repulsion–attraction forces, local activation and long-range inhibition, or motion in an external field; ref. 7), as well as specific examples that have rich pattern-forming features (8).

Patterns formed by organisms, and the way they shape their environment, is a rich area with physical (phase transitions), engineering (robotics), sociological (e.g., human traffic patterns), and ecological implications (5, 9–11). Social foraging in mixed-species groups and the emergent patterns of distributions have been studied in ecology (e.g., ref. 12). Rules of individual behavior in socially cohesive foraging and/or migrating groups have been explored recently in empirical and theoretical studies (13, 14).

In studying social foraging, our goal was to use a spatially explicit analytical framework. There is great interest in extending analytical and empirical studies to understanding the spatiotemporal dynamics of social aggregation, although tools for doing so are as yet emerging. Both individual-based models tracking single organisms (14) and density-based theories using partial differential equations (PDEs) (8, 17) contribute to such technology. The Keller–Segel (KS) model (18) provides a great avenue for exploration that already has a history to build on. This model is classical, based on a continuum approximation, and depicts a mechanism for spatial aggregation. Although explored in vast literature, KS has yet to be applied to the situation of dual social behavior here described, but see the individual-based model for gradient climbers and their highly social followers (14). Further, how organisms shape and are in turn affected by the spatial distribution of their resources is still an emerging area of research, addressed in this paper.

In group foraging studies, resource distribution, patch size and structure, and distance between foragers were shown to influence the "finders' share" (food obtained by producers vs. scroungers) (1, 15, 16), which motivated us to ask which strategy confers an advantage under various conditions. To do so, we ask how limited resource distribution, patch size, and movement/search parameters contribute to relative success, quantified by a ratio of net food consumed by foragers vs. exploiters. Recent spatially explicit simulations to explore this question were based on simulations of agent-based producer–scrounger models (1). Such studies suggest that social interactions should increase with decreasing patch encounter rate. These recent findings emphasize the need for spatially explicit approaches in social foraging theory.

We conclude by investigating how switching between strategies (within a generation) affects the relative abundance of each behavioral type. We also consider a similar question on the timescale of many generations, when success of each strategy determines reproductive fitness.

Taxis Models

To understand spatial aggregation patterns, modelers often formulate simple models that can be investigated analytically or computationally. Some models track single individuals, positing rules of interaction (1, 9) and others formulate equations to describe densities of populations. Most such models are PDEs (17) or (if nonlocal) integro-PDEs (20).

Author contributions: J.P.H. provided initial concept; N.T. performed analysis; N.T., B.V., J.P.H., and L.E.-K. designed research; N.T., B.V., J.P.H., and L.E.-K. performed research; and N.T., B.V., J.P.H., and L.E.-K. wrote the paper.

The authors declare no conflict of interest.

This article is a PNAS Direct Submission. M.A.L. is a guest editor invited by the Editorial Board.

[1]To whom correspondence should be addressed. E-mail: keshet@math.ubc.ca.

This article contains supporting information online at www.pnas.org/lookup/suppl/doi:10.1073/pnas.1201739109/-/DCSupplemental.

Typical taxis equations for the motion of a population $p(x,t)$ toward a concentration of chemical or food $c(x,t)$ have the form

$$\frac{\partial p}{\partial t} = D_p \nabla^2 p - \nabla \cdot [\chi_p p \nabla c], \qquad \textbf{[1a]}$$

$$\frac{\partial c}{\partial t} = D_c \nabla^2 c + h(c,p). \qquad \textbf{[1b]}$$

The first (Laplacian) terms describe random motion and/or chemical diffusion. Individuals also move by taxis up gradients of c with characteristic taxis parameter χ_p. In the KS model (18), individuals are amoeba and the chemical is cAMP, secreted by the cells and degraded at rate k. Hence the kinetic term is $h(c,p) = h_{\mathrm{KS}}(c,p) = \mu p - kc$. The KS model **[1]** and its variants have been thoroughly investigated in the mathematical and modeling literature. It is well known that the uniform steady state of such equations can be destabilized by small amplitude noise, giving rise to patterns of aggregation (18). A recent generalization to multiple species includes ref. 19.

Simple Foragers

Eq. **1** can be reinterpreted as prey taxis (PT) where foragers p move following the food concentrations c. Both foragers and their food prey also move randomly, with motility coefficients D_p and D_c, respectively. To represent a renewable resource that is consumed at rate $\hat{\lambda}$ per capita, decays at rate $\hat{m}$, and is replenished at rate $\hat{r}$, we typically chose the term $h(c,p) = h_{\mathrm{PT}}(c,p) = -\hat{\lambda} pc - \hat{m} c + \hat{r}$.

In 1D, with no immigration or emigration (no-flux boundary conditions on a domain of length L), the total forager population, $(\int_0^L p(x,t)dx)$ is constant. The model then has a spatially uniform steady state with a constant level of foragers and food everywhere.

In view of the rich mathematical theory for KS aggregation, it might be tempting to conclude that such prey–taxis systems can also aggregate, leading spontaneously to a patchy distribution of resources. This simple expectation is actually false, as argued in a comprehensive work in ref. 17. Intuitively, there is an important difference in the sign patterns of h_{KS} and h_{PT}: In KS, the individuals reinforce the chemical by secreting it (positive feedback), whereas in the prey–taxis, the consumption of prey depletes local patches (negative feedback).

In the *SI Appendix*, we show that the uniform steady state of **[1]** with $h = h_{\mathrm{PT}}$ is stable, so that any perturbation in the distribution of food and foragers decays with time. Deviations from uniformity get damped with time, and no instability (and hence no pattern formation) can arise. In the words of Lee et al. (17), "prey–taxis tends to transform heterogeneous environments into homogeneous environments, which gives an opposite result to the chemotaxis case," implying that simple prey–taxis does not lead to complex patch dynamics.

Foragers and Exploiters

We asked whether the presence of distinct species or behavioral types would alter the absence of spatiotemporal dynamics in the simple prey–taxis model. Consequently, we consider a mixed-species group with foragers that search for food directly, and others attracted to forager aggregations. Social foraging has been observed in a wide variety of taxa (2). It can include interactions among individuals of the same species, or information provided by exploiting discoveries of other species, such as in mixed-species foraging flocks (e.g., shearwater flocks that are attracted to kittiwake foragers in aquatic "catalyst-kleptoparasite" foraging flocks; ref. 12). Here, for simplicity, we focus on two types, termed simply "forager" and "exploiter," and consider both the static case and the case when individuals can switch between these strategies.

To model such a system, we extended and scaled the taxis model to track the fractional densities of foragers $p(x,t)$ and exploiters $s(x,t)$ (equivalently, producers and scroungers). The full (unscaled) equations are given in the *SI Appendix*. In their dimensionless form, these are

$$\frac{\partial p}{\partial t} = \nabla^2 p - \nu_p \nabla \cdot [p \nabla c] + h_p(p,s), \qquad \textbf{[2a]}$$

$$\frac{\partial s}{\partial t} = \nabla^2 s - \nu_s \nabla \cdot [s \nabla p] + h_s(p,s), \qquad \textbf{[2b]}$$

$$\frac{\partial c}{\partial t} = d \nabla^2 c - \lambda (p+s) c - \mu c + r. \qquad \textbf{[2c]}$$

Space has been scaled by the size of the domain (typical length, L) over which interactions occur and time by the timescale of random search over distance L. Dimensionless parameters ν_s, ν_p are relative taxis parameters of foragers and exploiters, $d = D_c/D_p$ is relative mobility of the prey, λ its per-capita consumption rate, and μ its decay rate. Food is replenished at rate r. The terms h_p and h_s, initially set to zero, allow us to consider switching between the two types. Details of the dimensionless parameters are given in the *SI Appendix*.

Interactions in a Fixed Patch with Distinct Species

We first study, the case of two distinct types that cannot switch behaviors so that $h_p = h_s = 0$ in Eq. **2**. For simplicity, we deal here with a 1D domain (scaled to unit length as above) with sealed ends, depicted by no-flux boundary conditions. Then the total population, $\int_0^1 p(x,t) + s(x,t)dx = 1$ is conserved, and we can explore dynamics for various choices of the fraction of foragers ϕ_p and exploiters $\phi_s = 1 - \phi_p$. From the structure of the model, it is clear that a spatially homogeneous steady state can exist, with populations uniformly distributed, $p(x) = \phi_p$ and $s(x) = 1 - \phi_p$, and the resource at level $c(x) = r/(\lambda + \mu)$. However, as argued below, this is not the only solution, and interesting dynamics can occur.

Forager-Exploiter Interactions Lead to Spatiotemporal Patterns and Patchy Resource Distribution

Standard linear stability analysis (LSA) of Eq. **2** reveals that the uniform steady state can be destabilized provided that

$$\frac{1}{(1-\phi_p)}\left[\frac{8(\lambda+\mu)^2(d+1)}{\nu_p \phi_p \lambda r} + 2(d+1)\right] \lesssim \nu_s. \qquad \textbf{[3]}$$

This condition can be interpreted as a threshold for the exploiter taxis parameter ν_s. When exploiters are weakly attracted to for-

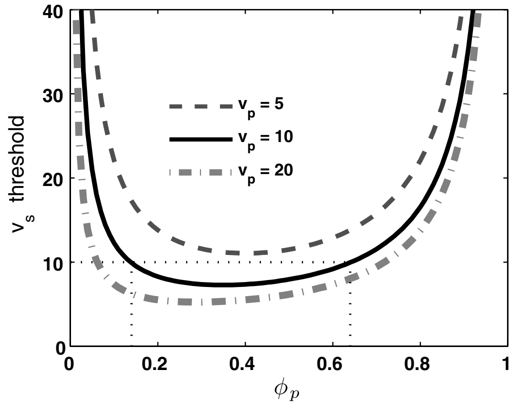

Fig. 1. Given the exploiter and forager taxis values ν_s, ν_p, only some intermediate fraction of foragers $\phi_1 < \phi_p < \phi_2$ can accommodate spatial instability **[3]**. Otherwise, $\phi_p < \phi_1$ provides insufficient cues for exploiter aggregation, and $\phi_p > \phi_2$, is like prey–taxis and supports no instability.

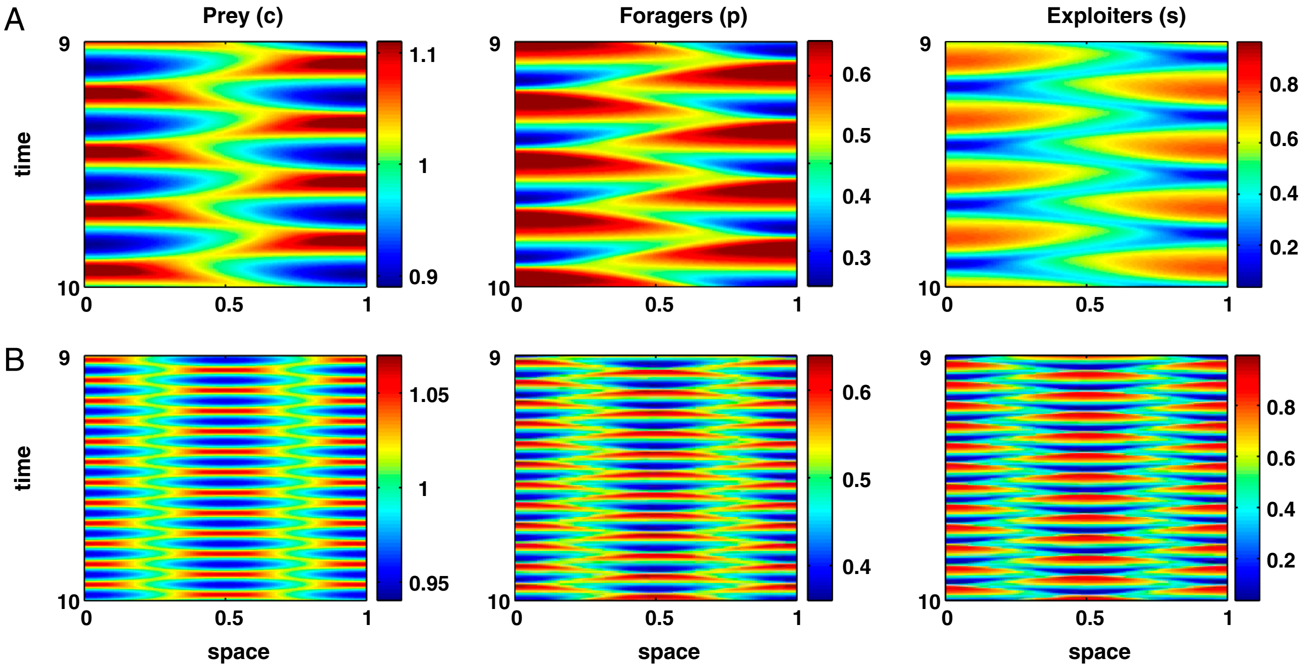

Fig. 2. Oscillatory spatial patterns in prey, forager, and exploiter densities for two values of exploiter taxis parameter v_s. Horizontal axis is space; vertical axis is time. Exploiter taxis parameter: (*A*) $v_s = 10$ and (*B*) $v_s = 20$. Other parameter values were $v_p = 10$, $\mu = 0.05$, $\lambda = 8.0$, $r = 8.05$, and $d = 0.1$.

ager groups (low v_s), instability is less likely, all else being equal. If v_s is large enough, inequality **[3]** implies that (*i*) increasing the mobility (through d) or decay rate of prey (through μ or the predation rate λ) is stabilizing, whereas (*ii*) increasing the prey–taxis coefficient (v_p) is destabilizing. Finally, (*iii*) the fraction of foragers (ϕ_p) also plays a role. We plot the left-hand side of [**3**] vs. ϕ_p in Fig. 1. Satisfying the inequality restricts ϕ_s to an intermediate range. For example, for $v_s = 10$ and $v_p = 10$, instability occurs for $0.14 \leq \phi_p \leq 0.64$.

We find that instability and spatial patterning is accompanied by temporal oscillations. (In the *SI Appendix*, we show that this instability stems from a Hopf bifurcation.) Linear stability analysis also predicts that, at some lower value of v_s, a single mode becomes unstable, whereas higher v_s allows for a range of unstable modes.

To visualize the resulting spatiotemporal dynamics, we carried out simulations of the system [**2**]. Fig. 2 shows the results for two values of v_s (Movies S1–S2). Starting from a nearly uniform distribution of foragers, exploiters, and resource, we observed growth of periodic waves. By $t = 9$, these fluctuations settle into regular cycles. For a smaller value of v_s (Fig. 2, *Upper*), a single "hot spot" (red) alternates between one and the other end of the domain. We can understand this behavior by noting that local aggregations of animals deplete the food, which takes time to renew. Meanwhile, movement toward undepleted food resources sets up growing fluctuations. It is these waves of pursuit that lead to the observed periodic fluctuation in the densities of the variables.

If the parameter v_s is increased (Fig. 2, *Lower*), the frequency of oscillation increases and a larger numbers of hot spots occur (resulting from instability of higher modes) with concurrent decrease in amplitudes of p and c. In the limit of high v_s, the system reduces back to the simple forager-resource system that has no spatial instability: This is the case in which the exploiters track foragers so efficiently that the motion of the two groups is practically indistinguishable. In this limit, the pattern can no longer be sustained, and only the spatially uniform state is stable.

So far, analysis and simulations were confined to 1D. We asked what the model predicts in higher dimension. This question is of interest because it is well-known that KS chemotactic equations can develop singularities and "blowup" solutions in finite time in 2D and 3D (21). We repeated this computation in 2D. As shown in the *SI Appendix* and Movies S3–S8, the oscillatory patterns of aggregation are also evident in the 2D setting. In contrast to the positive feedback in the KS model, here prey depletion serves as a negative feedback, preventing sharp peaks/singularities (due to aggregation) from occurring.

Advantages of the Strategies: Foraging Versus Exploiting

To compare the two strategies, we reasoned that at any given time, an individual of a given type has an opportunity to feed proportional to its per-capita contact with food—i.e., $c(x,t)p(x,t)/\phi_p$ or $c(x,t)s(x,t)/\phi_s$. We defined $F_p(t)$, $F_s(t)$ as the cumulative per-capita food intake for foragers and exploiters, respectively (obtained by integrating the contact rates over the domain, up to time t; see *SI Appendix* for details). Then the ratio $B(t) = F_s/F_p$ can be used to compare the relative advantage of the strategies. We also denote $b(t)$ as the ratio of instantaneous per-capita food intake—i.e., without integration over time. $B = 1$ implies both strategies are equally successful, whereas $B > 1$ corresponds to an advantage for exploiters. We consider both static and dynamic versions of this measure.

Relative Advantages for a Static Food Patch

We first considered a static spatially nonuniform food distribution $c(x)$ with analytically solvable steady-state forager/exploiter profiles $p(x)$, $s(x)$ and time-independent relative-advantage B. We chose a unimodal food distribution $c(x) = \cos(\pi x) + 1$ to satisfy no-flux boundary conditions for p and s. In Fig. 3, we numerically generated the curve of neutral advantage $B = 1$ in the v_p-v_s plane for various values of the forager fraction ϕ_p (see *SI Appendix*). Exploiters do best when (v_p, v_s) is above the curve vs. foragers below the curve. At a fixed forager acuity v_p, exploiters with v_s above some threshold have greater advantage. Foragers with low v_p are weakly attracted to food, so their density forms shallow gradients; then only exploiters with high acuity would detect such slight forager density gradients. For larger v_p, the foragers concentrate at food sources, forming sharper density gradients, so the threshold v_s value is lower. Larger ϕ_p shifts the $B = 1$ curve

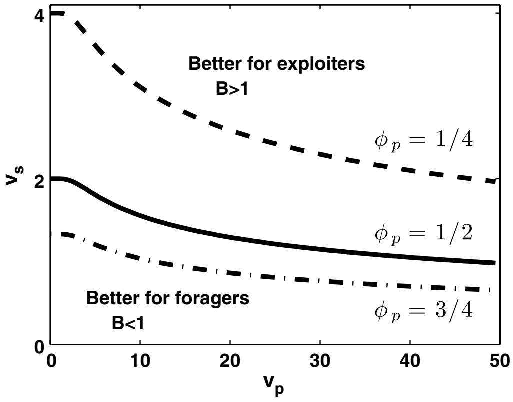

Fig. 3. Neutral curve ($B = 1$) for three values of ϕ_p. Above (below) the curve exploiters (foragers) have the advantage. [Figure credit, Marysa Lague.]

lower, so exploiters have the advantage ($B > 1$) for a wider range of v_s.

Relative Advantage for a Nonrenewable Resource

Next, we investigated relative advantage when food is depleted by consumption. Setting $r = 0$, $\mu = 0$ in [**2c**], we used Gaussian initial food profiles centered at $x = 0.5$, all with the same area ($\int c(x, 0)dx$), but varying standard deviation, σ. The "width" σ represents a typical food patch "size." About the populations, we assumed an initial uniform density of each type, with proportions $\phi_p, \phi_s = 1 - \phi_p$. We then asked how the relative success of the strategies varies with respect to key model parameters such as taxis rates v_s, v_p, relative prevalence of the two types, and patch size.

All else being equal, exploiters do better per capita when foragers are abundant, as in the static case. Hence B is an increasing function of ϕ_p (Fig. 4). Patch width affects the relative success. For wide food patches with shallow gradients (e.g., when $\sigma = 0.4$), both strategies are roughly the same ($B \approx 1$), regardless of the relative abundance of exploiters and foragers. For narrower patches with sharper gradients ($\sigma = 0.1, 0.05$), we find that $B < 1$, and foragers have a greater advantage over the whole range $0 \le \phi_p \le 1$.

We also explored how the foragers' ability to detect resource gradients affects the relative success of the strategies. Exploiters do poorly when their taxis parameter v_s is low relative to foragers' taxis parameter, v_p, because foragers can utilize and deplete the food before the arrival of exploiters (see *SI Appendix*, Fig. S1).

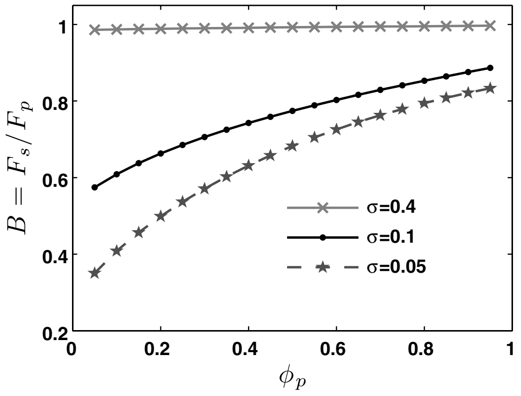

Fig. 4. Effect of the patch width σ and relative frequency of foragers ϕ_p on the relative advantage of the exploiter versus forager, $B = F_s/F_p = f(\phi_p, \sigma)$. Parameters as in Fig. 2 but with $r = 0$, $\mu = 0$. Initial conditions: Gaussian food distribution of width σ and uniform levels of foragers and exploiters.

In comparison to the static case, we found that, when resources are nonrenewable, foragers have the advantage for a wide range of parameter values ($B \le 1$ in Fig. 4 and *SI Appendix*, Fig. S1). This advantage stems from the fact that foragers are able to locate, consume, and deplete resources rapidly, before exploiters arrive. We then asked how two simple variations of the model might affect our conclusions.

1. We considered an energetic cost to primary foraging (e.g., finding or subduing prey) that exploiters avoid paying. Then the relative advantage becomes $B = F_s/(F_p - \text{cost})$. For sufficiently high cost, exploiters gain the advantage, $B > 1$, as expected (see *SI Appendix*, Fig. S2).
2. We also considered a mixed strategy, when exploiters also search for resources on their own (but with some reduced attention). To do so, we included a prey–taxis term in Eq. **2b** of the form $-(\alpha v_p)\nabla \cdot [s\nabla c]$, where $\alpha < 1$. In the *SI Appendix*, Fig. S3, we show that this variation allows for cases where $B > 1$ as well. Other variants (not here considered) that affect relative advantages could include more aggressive exploiters or differences in food consumption rates.

Finally, we asked whether and how the relative advantage varies over time for the full system as in Fig. 2. Results shown in Fig. 5 indicate that relative advantage fluctuates over the cyclic waves of pursuit. If exploiters taxis exceeds foragers' taxis ability, we find phases with $b > 1$, signifying times where exploiters temporarily do better than foragers.

Switching Between the Strategies

Thus far, populations of types p and s were fixed ($h_p = h_s = 0$ in Eq. **2**). However, both short-term plasticity (learning to switch strategy) and long-term dynamics (reproductive fitness) could lead to population changes. Understanding the implications of switching has been a key object of study in the social foraging literature (1, 22). Here we investigate both switching and adaptation in a spatial context, an important aspect, given that dynamic resource distributions might affect the relative benefits to exploiters and foragers dynamically (and distinctly) over time.

To consider dynamic behavioral switching, we assumed that $h_p = -h_s = \alpha(b)s - \beta(b)p$ with switching rates

$$s \to p: \ \alpha(b) = k/(1+b), \qquad p \to s: \ \beta(b) = kb/(1+b), \tag{4}$$

with k a maximal switching rate. Here the relative advantage b can be measured in terms of local, global, and finite sensing ranges, as detailed in the *SI Appendix*. Larger b favors $p \to s$ switching. For $b = 1$ (strategies equally successful), $\alpha = \beta = k/2$,

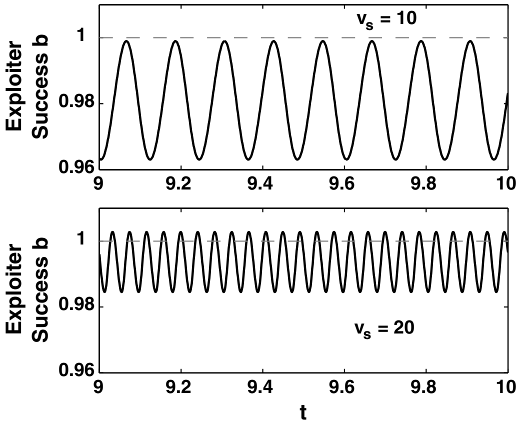

Fig. 5. Relative exploiter success $b(t)$ for two values of the taxis parameter $v_s = 10$ (*Upper*), $v_s = 20$ (*Lower*). Parameters and conditions as in Fig. 2.

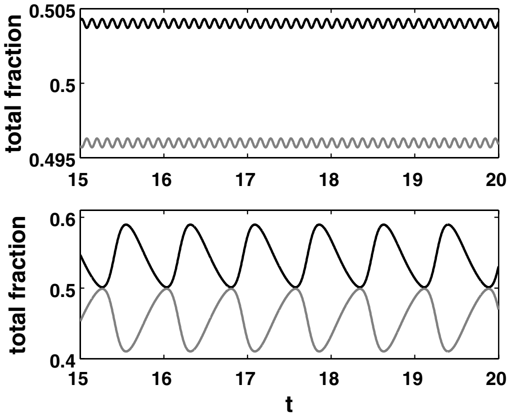

Fig. 6. The fractions of foragers and exploiters over time in the case of strategy switching. Parameter values as in Fig. 2, but with $v_p = 10$, $v_s = 10$, $k = 4$ (*Upper*), and $v_p = 1$, $v_s = 20$, $k = 19$ (*Lower*). Black curves indicate the fractions of foragers and gray curves for the fractions of exploiters.

the uniform steady state is $\phi_s = \phi_p$. Simulation results are shown in Fig. 6. For parameter values in Fig. 2, switching leads to hardly perceptible oscillations of strategies close to $p \approx s \approx 0.5$ (Fig. 6, *Upper*). Other parameter values, however, accentuate the cycles (Fig. 6, *Lower*; spatial patterns shown in *SI Appendix*, Fig. S7, and Movie S9). Such results reinforce the idea that spatial interactions can lead to behavioral transitions as well as dynamic forager-exploiter distributions. In contrast to a classic result where social interactions led to a fixed frequency of forager and exploiter (22), we observed temporal variations in the frequencies.

Further exploring the full spatiotemporal model, we found that switching can both promote or suppress instability, by shifting the critical v_s value at which oscillatory pattern emerges. Switching at constant rates, for example, yields new spatiotemporal patterns, not seen otherwise, including standing wave patterns (see *SI Appendix*, Fig. S6).

Next, we considered how reproductive fitness could affect the population structure over several generations. To do so, we omitted the short-term behavioral switching ($h_s = h_p = 0$), and assumed, instead, the semelparous reproduction rule

$$s(T+1) = F_s(T)/F(T), \qquad p(T+1) = F_p(T)/F(T), \qquad \mathbf{[5]}$$

for T the generation number, and $F = F_s + F_p$. Now **[2]** captures within-generation dynamics, whereas **[5]** relates reproductive fitness between generations to the relative success within a generation (while keeping population size fixed). Other cases with net population growth can be simulated by alternating the model of **[2]** (within a generation) with arbitrary fitness-based reproduction rule (see *SI Appendix*).

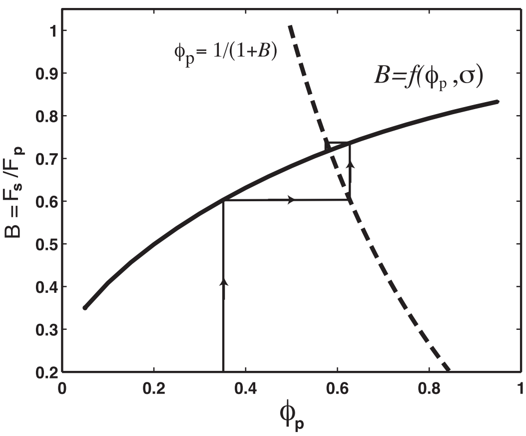

Fig. 7. When relative advantage of strategies affects the proportions of foragers and exploiters in the next generation (dotted curve), the fraction ϕ_p changes, here approaching a steady state. Solid curve: $f(\phi_p, \sigma)$, $\sigma = 0.05$ from Fig. 4.

Rewritten, **[5]** yields $\phi_p(T+1) = 1/[1 + B(T)]$ (dotted curve in Fig. 7). At each generation T, given $\phi_p(T)$, we can compute $B(T)$ by integrating food consumed by each strategy over the forager's lifespan. One such curve, $B(T) = F_s/F_p = f(\phi_p(T), \sigma)$ for σ-sized food patch shown in Fig. 4 is copied on Fig. 7 ($\sigma = 0.05$). Together, such two rules link intergenerational values of ϕ_p and B. A cobweb diagram based on this proof of principle illustrates convergence of ϕ_p to a unique stable equilibrium over several generations. Stable cycles are also possible, as discussed in the *SI Appendix*, Fig. S10, provided the function $f(\phi_p(T), \sigma)$ is steep enough. Thus, a variety of long-term dynamics are possible, and provide future directions to explore, based on various assumptions about the food, the fitness measure, and dynamics between and within generations.

Discussion

Social foraging models (2, 23) have addressed interactions in the context of information sharing (24) and frequency dependent dynamics (22, 25). One subset of such models examines so-called producer–scrounger systems wherein one species (the scrounger) exploits another (the producer). Most such investigations fail to account for spatially explicit interactions (16, 22, 25), which have been the focus of our paper.

Our results have two major thrusts. First, in a context of pattern formation, we revisited the classic prey–taxis model and showed that inclusion of exploiters leads to spontaneously emergent patterns (absent in the original model). Such results apply to a class of ecological models that fall under the rubric of producer–scrounger systems, although these have not been extensively studied in the literature. (One notable exception is Beauchamp, ref. 1, who indicated that spatial producer–scrounger systems could be self-organizing.) Using analytic techniques such as LSA, we found conditions on the parameters **[3]** for such patterns to occur, finding persistent spatiotemporal oscillations stemming from a Hopf bifurcation. These patterns form a stable attractor of the dynamics in both 1D (Fig. 2, Movies S1–S2) and 2D (Movies S3–S8). Heuristically, the primary foragers detect weak resource gradients, congregate, and form detectable "crowd gradients" to which exploiters respond. These interactions result in an inherent delay: It takes time for forager gradients to form in response to the prey distribution, and the exploiters can react only once such gradients are noticeable. This lag leads to waves of pursuit that arise spontaneously, with concomitant patchiness in the resource distribution.

In ecology, a common basic assumption is that resources are patchily distributed (26, 27) and that this influences competitive advantage of various strategies (28). Recent studies suggest that the amount of food obtained by producers vs. scroungers (the finders' share), can depend strongly on patch structure and distances between individuals (1, 15, 16). This idea motivated our second major thrust, to explore the relative benefits of the two social foraging strategies in the model. We quantified benefit in terms of resources available to each strategy. In the case of fixed strategies and static resource distribution, we found (using convenient closed-form solutions of the system) how relative success depends on the relative acuity and abundance of each species (taxis parameters v_s, v_p and forager fraction ϕ_p). For a fixed forager taxis parameter v_p, exploiters do better as v_s increases, or as the fraction of foragers ϕ_p (and hence the steepness of their gradient) increases. Exploiters also "win" at fixed intermediate values of v_s and small ϕ_p for large v_p, again due to sharp gradients of foragers they can detect. Both ideas relate to ways of crossing the neutral curve $B = 1$ shown in Fig. 3. In the case of exhaustible food patches, the strategies are equal only when resources are widely dispersed (large σ in a normally distributed resource patch). Otherwise, foragers arrive first, get a larger share, and have the advantage over exploiters.

We examined strategy switching based on the changing benefit to forager vs. exploiter, which was in turn related to the dynamics of prey patchiness. Both long- or short-ranged sensing of resources was considered. Overall, we found that switching created cycles of relative forager/exploiter abundance, whose frequency and amplitude depends on sensing ranges in a nontrivial manner. Whereas most classic approaches lead to a fixed frequency of producers and scroungers (22), here we have shown it to be dynamic, an important result. The interesting dynamics suggest avenues of future mathematical exploration.

Our study has features in common with Guttal and Couzin (14). They discuss a dichotomy of gradient-climbing "leaders" and social individuals ("followers") in an individual-based model of migration. Here we were not concerned with long-range migration and only hinted at possible evolutionary implications. Our use of PDEs led to analytic results. We also note the distinction of our patterns and the patchiness arising from diffusive (Turing based) instabilities in plankton, for example, ref. 4. The latter depends on simple dispersion, coupled with specific kinds of local predator–prey interactions.

We also tested extensions and variants of the basic model to check robustness of conclusions to the assumptions. The variants studied included (*i*) some weak additional attraction of exploiters to food, and (*ii*) attraction of exploiters to both forager and exploiter aggregates—i.e., taxis of the form $-v_s \nabla s \cdot \nabla(s+p)$. Overall, results are similar, and are omitted for brevity (but see *SI Appendix* for additional detail).

Results of this model can be applied to many systems that have inspired social foraging theory to date (23) as well as to systems where predators can shape the patchiness of their prey, e.g., shorebirds (29), plankton (4), or arctic eider ducks diving under sea ice for slow-moving benthic invertebrates (30). First, estimation of the taxis parameter v_p can be made using short-term movement measurements of foragers toward artificially created (known) resource gradients. Similar estimation of v_s for the exploiting species could be extracted under the same conditions. Fig. 1 then suggests experiments to manipulate relative abundance of the two species (from all foragers to all exploiters). Our results predict that, if spatiotemporal patterns occur, they should appear at some intermediate ratio of the two types, and not at the two extremes. The condition for pattern **[3]** also suggests that rapidly dispersing prey or highly mobile prey (large d) are inconsistent with spatial patterns.

The limitations of continuum taxis models are that structure and dynamics of food resources are restricted to smooth functions. The model predicts dynamics of large groups for whom densities are an adequate representation. At the same time, the strength of the approach is that it provides an analytical baseline for a spatial theory of frequency dependant foraging and aggregation. Further, building on established chemotaxis aggregation models, it adds a frequency-dependent dynamics that could provide general insights into pattern formation and self-organizing systems.

ACKNOWLEDGMENTS. N.T. and B.V. were supported by a Natural Sciences and Engineering Research Council (NSERC) discovery, and an accelerator grant (to L.E.-K.). J.P.H. has been supported by an NSERC Postdoctoral Fellowship. While conducting part of this research, L.E.-K. was a Distinguished Scholar in Residence of The Peter Wall Institute for Advanced Studies and supported by National Institutes of Health (R01 GM086882 to Anders Carlsson).

1. Beauchamp G (2008) A spatial model of producing and scrounging. *Anim Behav* 76:1935–1942.
2. Giraldeau LA, Caraco T (1999) *Social Foraging Theory* (Princeton Univ Press, Princeton).
3. Turing AM (1952) The chemical basis of morphogenesis. *Philos Trans R Soc Lond* 237:37–72.
4. Levin SA, Segel LA (1976) Hypothesis for origin of planktonic patchiness. *Nature* 259:659.
5. Levin S (1992) The problem of pattern and scale in ecology: The Robert H. MacArthur award lecture. *Ecology* 73:1943–1967.
6. Maini PK, Painter KJ, Chau HNP (1997) Spatial pattern formation in chemical and biological systems. *J Chem Soc Faraday Trans* 93:3601–3610.
7. Cross MC, Hohenberg PC (1993) Pattern formation outside of equilibrium. *Rev Mod Phys* 65:851–1112.
8. Eftimie R, De Vries G, Lewis MA (2007) Complex spatial group patterns result from different animal communication mechanisms. *Proc Natl Acad Sci USA* 104:6974–6980.
9. Vicsek T, Czirók A, Ben-Jacob A, Cohen I, Shochet O (1995) Novel type of phase transition in a system of self-driven particles. *Phys Rev Lett* 75:1226–1229.
10. Payton D, Daily M, Estowski R, Howard M, Lee C (2001) Pheromone robotics. *Auton Robots* 11:319–324.
11. Helbing D, Schweitzer F, Keltsch J, Molnar P (1997) Active walker model for the formation of human and animal trail systems. *Phys Rev E Stat Nonlin Soft Matter Phys* 56:2527–2539.
12. Hoffman W, Heinemann D, Wiens JA (1981) The ecology of seabird feeding flocks in Alaska. *Auk* 98:437–456.
13. Lukeman R, Li YX, Edelstein-Keshet L (2010) Inferring individual rules from collective behavior. *Proc Natl Acad Sci USA* 107:12576–12580.
14. Guttal V, Couzin ID (2010) Social interactions, information use, and the evolution of collective migration. *Proc Natl Acad Sci USA* 107:16172–16177.
15. Barta Z, Flynn R, Giraldeau L (1997) Geometry for a selfish foraging group: A genetic algoritm approach. *Proc R Soc London Ser B* 264:1233–1238.
16. Ohtsuka Y, Toquenaga Y (2009) The patch distributed producer-scrounger game. *J Theor Biol* 260:261–266.
17. Lee JM, Hillen T, Lewis MA (2009) Pattern formation in prey-taxis systems. *J Biol Dyn* 3:551–573.
18. Keller EF, Segel LA (1970) The initiation of slime model aggregation viewed as an instability. *J Theor Biol* 26:399–415.
19. Horstmann D (2011) Generalizing the Keller-Segel model: Lyapunov functionals, steady state analysis, and blow-up results for multi-species chemotaxis models in the presence of attraction and repulsion between competitive interacting species. *J Nonlinear Sci* 21:231–270.
20. Green JEF, et al. (2010) Non-local models for the formation of hepatocyte-stellate cell aggregates. *J Theor Biol* 267:106–120.
21. Hillen T, Painter K (2001) Global existence for a parabolic chemotaxis model with prevention of overcrowding. *Adv Appl Math* 26:280–301.
22. Vickery WL, Giraldeau L, Templeton J, Kramer D, Chapman C (1991) Producers, scroungers and group foraging. *Am Nat* 137:847–863.
23. Giraldeau LA, Beauchamp G (1999) Food exploitation: Searching for the optimal joining policy. *Trends Ecol Evol* 14:102–106.
24. Clark CW, Mangel M (1984) Foraging and flocking strategies: Information in an uncertain environment. *Am Nat* 123:626–641.
25. Barnard CJ, Sibly RM (1981) Producers and scroungers: A general model and its application to captive flocks of house sparrows. *Anim Behav* 29:543–550.
26. Wiens JA (1976) Population responses to patchy environments. *Annu Rev Ecol Syst* 7:81–120.
27. Kareiva P, Mullen A, Southwood R (1990) Population dynamics in spatially complex environments: Theory and data [and discussion]. *Philos Trans R Soc* 330:175–190.
28. Hanski I (1983) Coexistence of competitors in patchy environment. *Ecology* 64:493–500.
29. Schneider DC (1992) Thinning and clearing of prey by predators. *Am Nat* 139:148–160.
30. Heath JP, Gilchrist HG, Ydenberg R (2010) Interactions between rate processes with different timescales explain counterintuitive foraging patterns of arctic wintering eiders. *Proc R Soc London Ser B* 277:3179–3186.